Int. J. Electrochem. Sci., 11 **(2016)** 4712 – 4723, doi: 10.20964/2016.06.83

International Journal of
ELECTROCHEMICAL
SCIENCE
www.electrochemsci.org

Synthesis of Copper Nanoparticles with Various Sizes and Shapes: Application as a Superior Non-Enzymatic Sensor and Antibacterial Agent

EmanAlzahrani[1,*], *Rasha A. Ahmed*[1,2,*]

[1]Chemistry Department, Faculty of Science, Taif University, 888-Taif, Kingdom of Saudi Arabia.
[2]Forensic Chemistry Laboratories, Medico Legal Department, Ministry of Justice, Cairo, Egypt.
[*]E-mail: em-s-z@hotmail.com, rashaauf@yahoo.com

Received: 7 February 2016 / *Accepted:* 5 April 2016 / *Published:* 4 May 2016

Copper nanoparticles (CuNPs) play an important role in optics, electronics, and antimicrobial fields. In this work we reported, synthesized CuNPs with various sizes and shapes by a facile chemical reduction of copper nitrate $Cu(NO_3)_2$ solution using isopropyl alcohol (IPA) as a reducing agent and cetyltrimethyl ammonium bromide (CTAB) as a capping agent. The relationships between the $Cu(NO_3)_2$ and CTAB concentration ratios and the size of the CuNPs were elucidated by optical measurements. It was found that at a high CTAB concentration, hexagonal CuNPs were formed. In contrast, at a high concentration of copper nitrate, spherical CuNPs were formed in aggregations. From the TEM analysis, it was found that the CuNPs exhibit three different sizes (16, 23, and 37 nm), which displayed characteristic adsorption bands at 551-572 nm. The electrocatalytic activities of the CuNPs with different sizes and shapes towards H_2O_2 were systematically explored, and it was found that the electrocatalytic activity was strongly dependent on the microstructure of CuNPs, through changing the oxidation current values of the CuNPs. The cyclic voltammetry results showed that ratio 1:2 CTAB: $Cu(NO_3)_2$ exhibited good electrocatalytic activity than other ratios. Furthermore, the proposed sensor demonstrated significant antibacterial activities against gram-negative (*E. coli*) more than gram-positive (*S. aureus*) bacteria. In summary, this work demonstrates a facile, economic and fast method for the fabrication of copper nanoparticles with high catalytic activity using CTAB/IPA, which have potential as a non-enzymatic sensor for H_2O_2 detection and could be used in biomedical applications.

Keywords: Copper nanoparticle; CTAB; Modified electrode; Electrochemistry; H_2O_2 detection; Antimicrobial.

1. INTRODUCTION

In the present century, nanotechnology has been widely used in many fields, due to its ability to change the structure of molecules at the atomic level. Crucial challenges surround the synthesis of

metal nanoparticles, which have superior properties to that of the bulk structure; for instance, metallic nanoparticles exhibit superior optical [1], electronic [2], magnetic [3], thermal [4], and sensing functionalities [5].

Among various metal nanoparticles, CuNPs is an important semiconductor with a band gap of 2.1 eV, has been paid much attention in recent years because of its intrinsic properties and wide potential applications in many fields such as photochemical catalysis, biosensing, gas sensor, electrochemical sensing and solar/photovoltaic energy conversion [1-4]. The synthesis of CuNPs has been achieved via various routes, including chemical reduction [6, 7], thermal decomposition [8, 9], the polyol method [10, 11], reverse micelles [12, 13], electron beam irradiation [14], micro-emulsion techniques [15], wire explosion [16] and *in situ* chemical synthesis [17].Taking into account the spontaneous oxidation of copper, those methods were performed in non-aqueous media. Among all the procedures, using a compound with the ability to form a complex with metal ions, such as soluble polymers or surfactants, is considered an attractive method for the synthesis of CuNPs, as it prevent the nanoparticles from agglomerating during the synthesis process [18-22]. As it is well known, shape, size and microstructures are the main factors that determine the chemical and physical properties of nanomaterials. Thus, these can be changed by fine tuning the surfactant concentration, which acts as an effective stabilizer/growth controller [23-25]. Unfortunally, there is a lack of understanding of the size effect in the electrocatalytic activity. Therefore, studying the influence of the size of copper nanoparticles on its electrochemical properties is of great importance and desirable.

Research on the quantitative detection of H_2O_2 has been given considerable attention, since H_2O_2 is a common oxidizing agent and an essential intermediate in biomedical, pharmaceutical, industrial and environmental protection and electrochemistry. Many traditional techniques have been employed to detect H_2O_2[26-30]. Among those techniques, non-enzymatic electrodes-based electrochemical method holds a leading position among various techniques. Therefore, CuNPs demonstrate excellent performance in glucose oxidation or H_2O_2 reduction sensors [31] due to their morphology, high specific surface area, good electrocatalytic activity and the possibility of promoting electron transfer reactions at a lower over potential [32].

In recent years, the synthesis and utilization of novel antimicrobial metal nanoparticles has increased due to the gradual increase of drug resistance among microorganisms. For this reason, copper compounds have also been employed as antimicrobial and antifungus agents. By using nanotechnology, which enhances the antimicrobial activity of copper metal by manipulating it to the nanoparticles, CuNPs have been widely used to control fungal crop diseases as well as acting as a disinfectant on farms [33, 34].

In this work, we synthesize the CuNPs of different shapes and sizes by a facile method. To compare the electrocatalytic activity of the CuNPs with three different shapes, we designed an enzymeless H_2O_2 sensor by direct deposition of the CuNPs on a bare glassy carbon electrode (GCE) surface. By analyzing cyclic voltammograms (CVs), the influences of CuNPs shape and size on electrocatalytic properties toward H_2O_2 were investigated. Moreover, the adsorption efficiency of the fabricated CuNPs was studied using a UV-Vis spectrophotometer. In addition, the morphology and the size of the nanoparticles were studied using transmission electron microscopy (TEM). Finally, the

antimicrobial activity against (*E. coli*) and (*S. aureus*) bacteria by a well disk diffusion assay was performed.

2. MATERIALS AND METHODS

2.1. Materials

Copper(II) nitrate ($Cu(NO_3)_2$), isopropyl alcohol (IPA) and cetyltrimethyl ammonium bromide (CTAB) were purchased from Sigma-Aldrich (Poole, UK). H_2O_2 solution (30 wt%) was purchased from Sinopharm Chemical Reagent Co., Ltd (Beijing, China). 1 M H_2O_2 solution was prepared and kept in the dark. All other chemical reagents were analytical grade and used as received without further purification. Phosphate buffer solutions (PBS) were prepared with 0.1 M K_2HPO_4 and KH_2PO_4 using 0.1 M KCl. Double-distilled water was used for preparing the aqueous solutions.

2.1.2. Synthesis of the CuNPs

The synthesis of homogenous and stable CuNPs with different shapes and sizes was achieved by the reduction of copper (II) nitrate with IPA in the presence of the cationic surfactant (CTAB) by the following method: 0.1 mM of copper (II) nitrate and 1 mM of CTAB were prepared in IPA. Copper (II) nitrate solution was added dropwise to the reductant solution of CTAB/(IPA) in three different ratios (2:1, 1:1, 1:2) under rapid stirring (700 rpm) at room temperature. The blue solution of cupric nitrate turned violet then darker violet, indicating the synthesis of the CuNPs [35].

2.1.3. Characterization of the CuNPs

Optical analysis and the spectra of the CuNPs synthesized from the three mixtures of $Cu(NO_3)_2$ and CTAB in IPA were recorded using a UV-Vis spectrophotometer at the resolution of 1 nm from 450 to 650 nm for each ratio compared to $Cu(NO_3)_2$ as a control solution. The morphology and the microstructure of the synthesized CuNPs were studied by transmission electron microscope.

2.1.4. Antibacterial activity assessment

The antibacterial activity of the CuNPs was tested against gram-positive –*Staphylococcus aureus (S. aureus*) – bacteria, and gram-negative – *Escherichia coli (E.coli)* – using the agar disc-diffusion method. A sterile paper disc (diameter 5 mm) containing CuNPs prepared using different ratios of CuNPs/CTAB were placed on the plates. The plates were incubated at 37 ºC for 24 h, and then the zone of inhibition (clear areas) around the discs was measured.

2.1.5. Preparation of CuNPs/GC for catalytic activity

Various CuNPs/GC electrodes were prepared by dipping a GC electrode into the different ratios of CuNPs/CTAB (IPA) and left to dry for 15 min at room temperature. The catalytic activity of the CuNPs/CTAB (IPA) was examined in the absence and presence of 1 M of H_2O_2 from +0.2 to -0.8 V at a scan rate of 10 mV s^{-1} in N_2-saturated PBS (0.1 M, pH 7.4).

2.2. Instrumentation

A magnetic stirrer from VWR International LLC (West Chester, PA, USA) and a UV-Vis spectrophotometer from Thermo Scientific™ GENESYS 10S (Toronto, Canada) was used for the spectrophotometric measurements.

The morphology and microstructure of the synthesized CuNPs were studied using a transmission electron microscope from JEOL Ltd. (Welwyn Garden City, UK) with an accelerating voltage of 20 kV and with different magnifications up to X 2000.

The electrochemical analysis was performed, using a potentiostat/galvanostat (Model 73022, Autolab Instruments, Metrohm) with a standard three-electrode cell to examine the reduction potential of the CuNPs. Ag/AgCl electrode, platinum wire and GC electrode were used as the reference, counter and working electrodes, respectively. The cyclic voltammograms (CVs) were measured at room temperature by using an aqueous solution containing $Cu(NO_3)_2$ (0.1 mM) dissolved in 1 mM CTAB solution dissolved into isopropyl alcohol, and scanned at a scan rate 50 mV s^{-1} from -1.0 V to +1.0 V.

3. RESULTS AND DISCUSSION

3.1. Mechanism of action

CuNPs were synthesized at various concentrations ratios of the precursor copper and CTAB. A chemical reduction method was used employing IPA as the reducing agent, as it can instantaneously produce a large number of nucleation centers and hence smaller particles. On the addition of $Cu(NO_3)_2$ solution to CTAB, the solutions turned dark violet, indicating the formation of CuNPs. The color change was due to surface plasmon resonance (SPR) [35].

It is well known that the critical micellar concentration (CMC) of CTAB is $\sim 9\times10^{-4}$ M, while for CuNPs it is $\sim 1\times10^{-3}$ M [36]. The mechanism of CuNPs formation is different at various concentration ratios. It was found that at a high concentration of $Cu(NO_3)_2$, (above its CMC) compared to CTAB, various aggregates of spherical CuNPs surrounded by monolayer copper oxide were observed. The formation of various aggregates was attributed to the high concentration of Cu^+ ions covered by a monolayer of CTAB molecules adsorbed on their surface. This monolayer does not have the ability to overcome the high van der Waals attraction between Cu^+ ions causing those aggregates. Spherical particles of CuNPs have a diameter of $\sim$37 nm with an absorption peak at $\sim$551 nm (the details are discussed in a later section). While a high concentration of CTAB, (above its CMC) with

respect to copper(II) nitrate concentration, provides more Br^- ions. In this case, large micelles of Br^- were formed around the Cu^+, thus pure CuNPs were formed with no copper oxide particles.

Micelle formation induces an increase in the local copper concentration at the interface. Fast reduction by the IPA causes a large number of metallic copper nuclei to form instantaneously. The presence of large numbers of micelles prevents particle growth and thus restricts the aggregation of the CuNPs. Thus surfactant micelles help to arrest nanoparticle growth and restrict them to a small, hexagonal shape [37]. The resultant nanoparticles possess a small diameter of 23 nm with a hexagonal shape. This is accompanied by a decrease in the intensity of the absorption peak, which is recognized at 572 nm.

3.2. UV-visible spectroscopy

The fabricated CuNPs were studied by optical measurements using a UV-Vis spectrophotometer over the wavelength range of 450-650 nm.

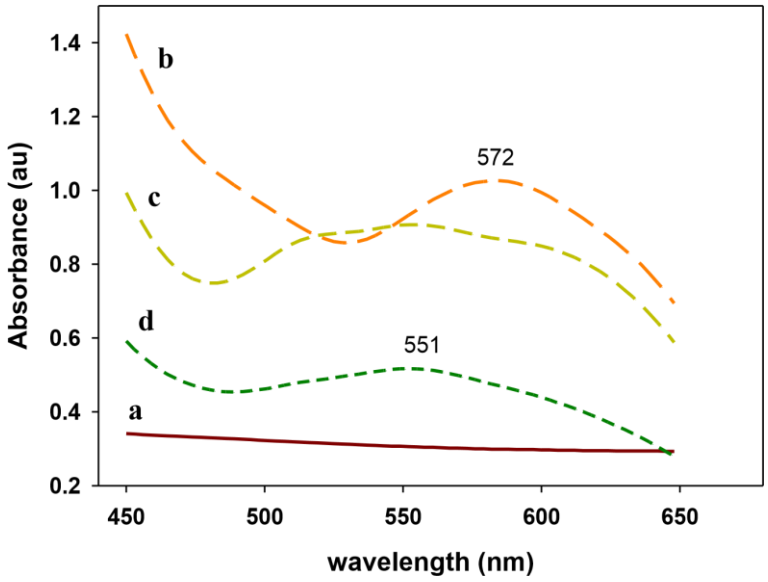

Figure 1. UV-Vis Absorption Spectra of (a) $Cu(NO_3)_2$ as a blank, (b)2:1, (c)1:1, (d)1:2 different concentration ratios of CTAB and $Cu(NO_3)_2$solution, respectively.

Fig.1 depicts the UV-Vis spectra of the fabricated CuNPs, with a blank peak for $Cu(NO_3)_2$ in Fig. 1a. It was noticed that all the three observed peaks were around 572 nm, but their intensities were affected by the CTAB and copper concentration ratios. Firstly, at a ratio 2:1 of CTAB: Cu $(NO_3)_2$, the absorption intensity was enhanced at 572 nm, due to formation of stable nanoparticles (Fig. 1b). At equal ratio of the precursor copper and CTAB was 1:1, absorption intensity was decreased with the appearance of a broad adsorption peak in Fig. 1c. This was attributed to the formation of the overlap between two peaks at 518 nm and 553 nm [38, 39]. The first peak is attributed to single non-aggregated nanoparticles in solution while the second is attributed to larger nanoparticles. It is

noticeable that in Fig. 1d, an absorption peak was formed at 551 nm with a remarkable decrease in intensity, for the CTAB:$Cu(NO_3)_2$ ratio of 1:2. This affirms the existence of copper oxide with copper nanoparticles. The results obtained by UV-Vis Absorption Spectra were confirmed by using TEM.

3.3. TEM analysis

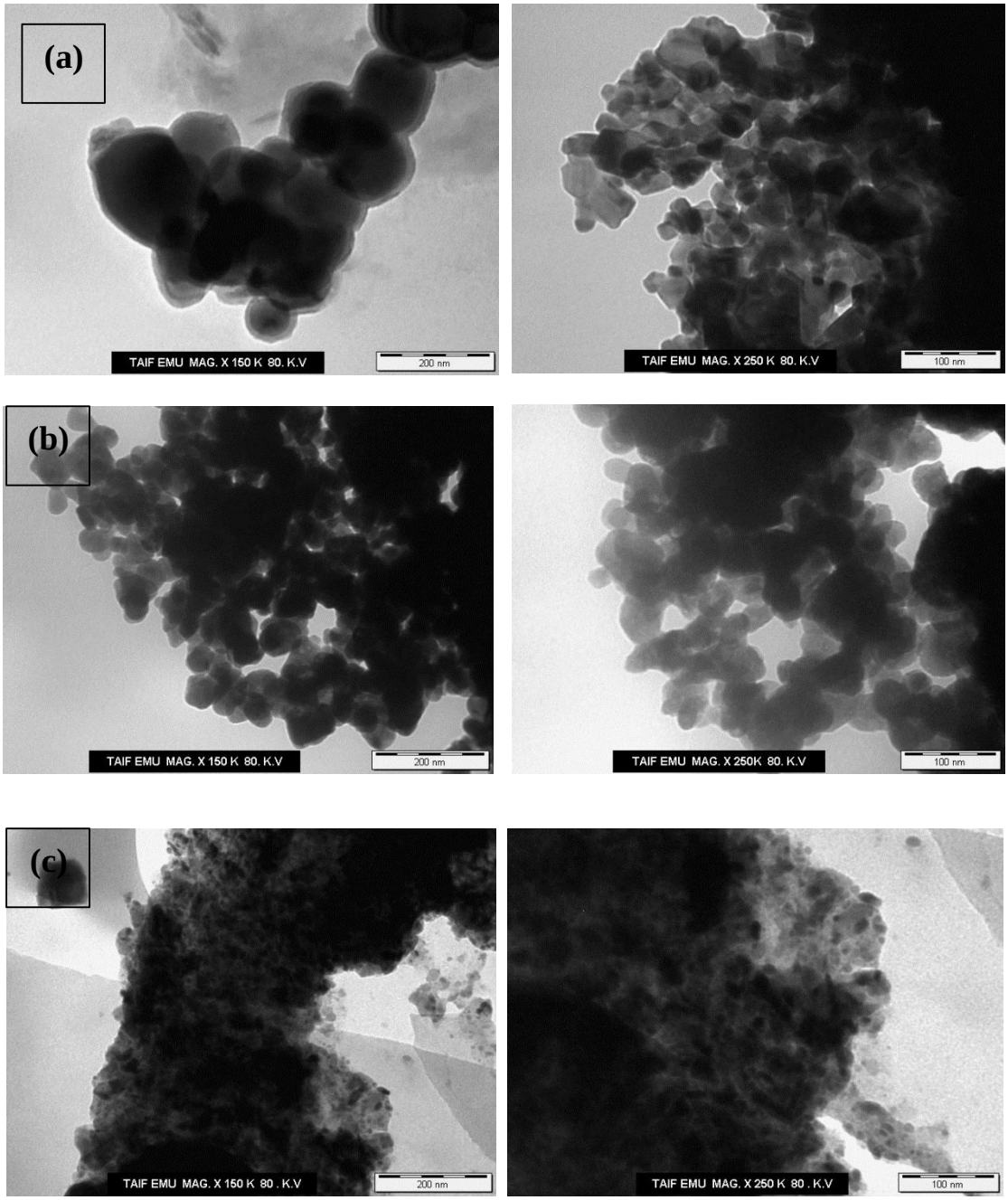

Figure 2. TEM images of CuNPs prepared using different ratios of $Cu(NO_3)_2$ and CTAB (a) 2:1, (b) 1:1, and (c) 1:2.

In this study, the fabricated CuNPs using different ratios of precursor copper and CTAB were characterized using TEM analysis, since it can provide information about the morphology and size of the fabricated nanoparticles.

TEM image of the CuNPs (Fig. 2a) synthesized using a 2:1 ratio CTAB:$Cu(NO_3)_2$ showed that the particles formed are small in size at approximately 23 nm, and were not perfectly round in shape, with the particles seen to be hexagonal in shape. For the ratio of 1:2 CTAB:$Cu(NO_3)_2$, in Fig. 2b, the TEM result illustrated the presence of 37 nm CuNPs, which appeared spherical in shape. Fig. 2c shows the TEM image of the CuNPs prepared using a 1:1 ratio of CTAB:$Cu(NO_3)_2$, which shows spherical particles in the range of 16 nm. In addition, it was observed that these nanoparticles were overlapping with each other, thus forming aggregates [39]. These results confirmed that the sizes and shapes of CuNPs were affected by the ratio between CTAB and $Cu(NO_3)_2$, which influences the growth rate of the nanoparticles. The results come in a good agreement with the UV-Vis absorption Spectra.

3.4. Electrochemical behavior of different size CuNPs

Cyclic voltammetry was employed to study the conductivity performance through alternation of the intensity of the oxidation and reduction current peaks according to the concentration ratio of the precursor copper and CTAB/IPA, in their solutions (0.1 mol L^{-1} at pH 7.0) with a potential window of −1.00 to 1.00 V and at a scan rate of 50 mV s^{-1}.

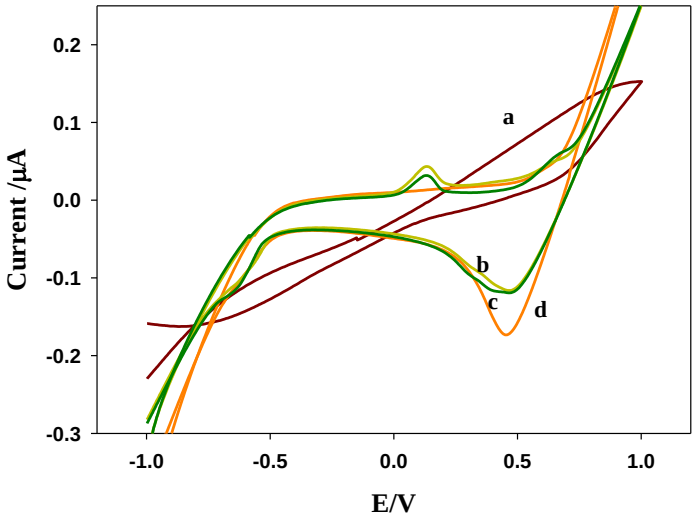

Figure 3. CVs for bare GC in CTAB: $Cu(NO_3)_2$ solution with ratio (a) 2:1 (b)1:1 (c)1:2, with scan rate 50 mV/s.

Fig.3 (a-d) illustrates the CVs of the bare GC electrode; and 2:1, 1:1, 1:2 precursor copper and CTAB, respectively. As can be seen from Fig. 3a, CTAB did not show any oxidation/reduction peak with the GC electrode, while Fig. 3 (b,c) presents a couple of well-defined redox peaks that were

observed at + 0.1 and +0.45 V. This was due to the Cu^{2+}/CuNPs redox behavior [40]. Furthermore, different current intensities were observed due to the different shapes and sizes of the CuNPs formed. Current values were found to be more intense in the following order: 2:1 > 1:2 > 1:1. CuNPs formed from equimolar concentration had the lowest oxidation current value, followed by the hexagonal-shaped CuNPs; however, by mixing a high concentration of CTAB with copper (II) nitrate, the spherical-shaped CuNPs showed a better conductivity performance than the others.

3.5. Applications of CuNPs

3.5.1. Antibacterial activity studies

Recently, the use of metal nanoparticles against bacteria has increased because of the gradual increase in drug resistance among microorganism [41]. In the present study, the fabricated nanoparticles were tested for antibacterial activity against human pathogenic bacteria, namely, *E coli* and *S. aureus*, by the agar disc diffusion method, and a Luria Bertani (LB) broth/agar medium that was utilized to cultivate the bacteria.

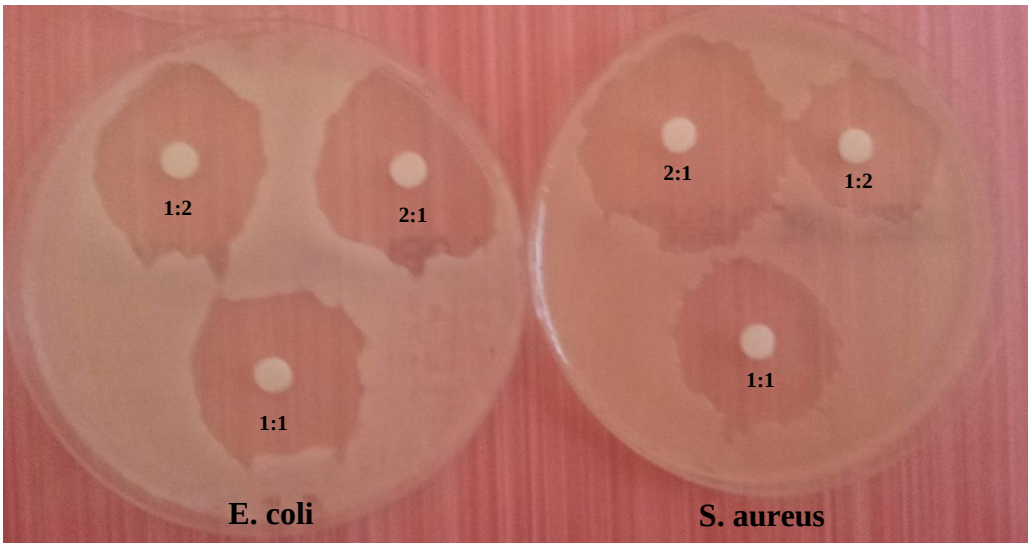

Figure 4. Zone of inhibition around discs impregnated with copper nanoparticles prepared using different ratio of copper (II) nitrate solution to CTAB against *E. coli* and *S. aureus*.

Fig.4 shows a clear inhibition zone of *S. aureus* and *E. coli* by the prepared CuNPs. It was concluded that the fabricated CuNPs had superior antibacterial activity to gram-positive and gram-negative bacteria. Although the exact mechanism of inhibition by the nanoparticles on the microorganisms is not clear, the antibacterial activity of CuNPs is clearly high due to their small size and high surface area to volume ratio (S/V), which allows them to interact closely with the membranes of the microbe. In addition, the surface of the nanoparticles interacts with the bacterial outer membrane, resulting in capture of the membrane and killing of the bacteria [42, 43].

From the figure, it can be observed that the CuNPs had more effect against gram negative bacteria (*E. coli*) compared with gram-positive bacteria (*S. aureus*). Several researchers found that the antibacterial effect was more pronounced against gram negative bacteria than gram-positive bacteria. This could be due to the interaction of the CuNPs and the cell wall of the bacteria facilitated by the abundance of negative charges on the gram-negative bacteria [42]. Moreover, the extent of the inhibition of bacterial growth in this study was affected by the concentration ratio of the surfactant and copper precursor. It was found the highest inhibition zone was obtained when the ratio of copper (II) nitrate solution and surfactant in the reaction mixture was 2:1.

3.5.2. Electrocatalytic activity

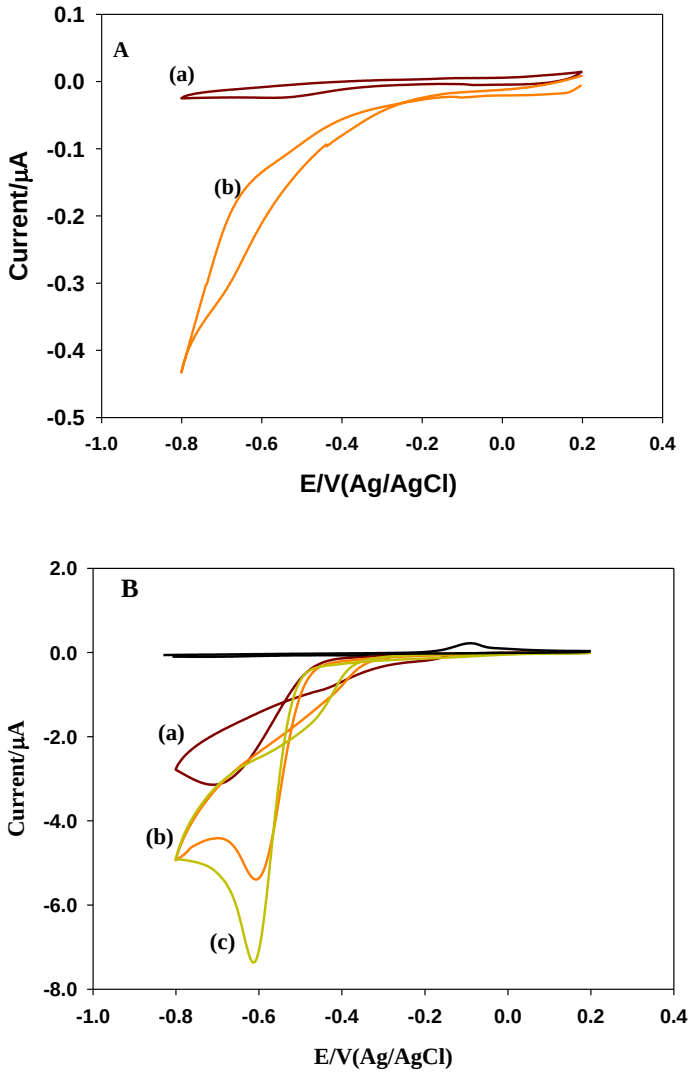

Figure 5. CVs for (A) bare GC (a) PBS and (b) 1 M H_2O_2; (B) Modified GC with CTAB: $Cu(NO_3)_2$ layer from ratio (a) 2:1, (b) 1:1, (c) 1:2 in 1 M H_2O_2 solution and in PBS (as a reference) with scan rate 10 mV/s.

H_2O_2 is a chemical used widely in the food, pharmaceutical, paper, and chemical industries. It is also a by-product of the reaction catalyzed by a large number of oxidase enzymes. The precise and rapid detection of H_2O_2 is of practical significance for both biochemical and environmental applications. Hydrogen peroxide (H_2O_2) was selected to check the applicability of the CuNPs/CTAB(IPA) electrode using cyclic voltammetry.

Fig. 5 (a, b) shows the CVs of GC and CuNPs/CTAB(IPA)/GC, respectively, in 0.1 mol L^{-1} PBS (pH: 7.0) in the absence and presence of 1 mol L^{-1} H_2O_2 at a scan rate of 10 mV s^{-1}. It can be obviously seen that the bare GC electrode represented no significant changes in PBS buffer solution, while a small reduction current response was observed in the presence of 1 M H_2O_2 (Fig. 5a). In the contrary, in Fig. 5b, the CuNPs/GC electrode showed an oxidation current peak at 0.19 V in buffer solution, this was attributed to the presence of a layer of CuNPs covering the GC electrode. Furthermore, it can be found that in the presence of H_2O_2, the CuNPs/CTAB(IPA)/GC electrode exhibited an obviously sharp reduction current peak for the three ratios [40], because of the adsorption of H_2O_2 on the electrode surface, resulting in the formation of the hydroxide ion (OH^-) then formation of H_2O.

The current intensities observed in the GC electrode modified with CuNPs/CTAB(IPA) were enhanced 20 fold more than that with the bare GC electrode. The experimental result demonstrated that CuNPs played an important role in the electrocatalytic performance of the electrode by enhancing both the adsorption ability and the electron transfer property, which is important for the reduction of H_2O_2 [44-45]. Furthermore, the reduction current peak was found to be sharper and more intense in the following order: 2:1 > 1:2 > 1:1. CuNPs formed from an equimolar concentration had the lowest reduction current value and a low efficiency for H_2O_2 catalytic reduction, then the hexagonal-shaped CuNPs; however, by mixing a high concentration of CTAB with copper (II) nitrate, the spherical-shaped CuNPs showed better performance in the catalytic reduction of H_2O_2 than the others. These results suggested that although the GC electrode alone demonstrated low electrocatalytic activity, CuNPs/CTAB(IPA)/GC could greatly enhance the electrocatalytic performance for H_2O_2 reduction.

4. CONCLUSION

In summary, the synthesis of CuNPs was achieved by the reduction of copper (II) nitrate in CTAB/IPA solution. The synthesized CuNPs were characterized by TEM analysis, UV-Vis spectroscopy and electrochemical techniques. TEM images revealed that the CuNPs were hexagonal or spherical in shape, with a size range of 16-37 nm, depending on the ratio between copper (II) nitrate and CTAB/IPA. We successfully constructed a non-enzymatic sensor for H_2O_2 determination based on CuNPs/CTAB (IPA). The electrochemical results showed reversible peaks for Cu^{2+}/CuNPs redox behavior. Moreover, the CuNPs synthesized in the present study showed promising antibacterial activity against *S. aureus* and *E. coli*, which could be attributed to their large surface area to volume ratio. This research demonstrated how the size of CuNPs has a significant effect on the reduction of hydrogen peroxide.

References

1. P. Zijlstra, M. Orrit, *Reports on Progress in Physics*, 74 (2011) 106401.
2. A. Kamyshny, J. Steinke, S. Magdassi, *Open Applied Physics J.*, 4 (2011) 19.
3. R. Gréget, G.L. Nealon, B. Vileno, P. Turek, C. Mény, F. Ott, A. Derory, E. Voirin, E. Rivière, A. Rogalev, *ChemPhysChem*, 13 (2012) 3092.
4. R.R. Letfullin, C.B. Iversen, T.F. George, *Nanomedicine: Nanotech., Bio. and Med.*, 7 (2011) 137.
5. G. Doria, J. Conde, B. Veigas, L. Giestas, C. Almeida, M. Assunção, J. Rosa, P.V. Baptista, *Sensors*, 12 (2012) 1657.
6. P. Khanna, S. Gaikwad, P. Adhyapak, N. Singh, R. Marimuthu, *Materials Letters*, 61 (2007) 4711.
7. H. Hashemipour, M.E. Zadeh, R. Pourakbari, P. Rahimi, *Inter. J. of Physical Sciences*, 6 (2011) 4331.
8. M. Salavati-Niasari, F. Davar, *Materials Letters*, 63 (2009) 441.
9. Y.H. Kim, D.K. Lee, B.G. Jo, J.H. Jeong, Y.S. Kang, *Colloids and Surfaces A: Physicochemical and Eng. Aspects*, 284 (2006) 364.
10. K. Woo, D. Kim, J.S. Kim, S. Lim, J. Moon, *Langmuir*, 25 (2008) 429.
11. B.K. Park, D. Kim, S. Jeong, J. Moon, J.S. Kim, *Thin Solid Films*, 515 (2007) 7706.
12. M. Pileni, I. Lisiecki, *Colloids and Surfaces A: Physicochem. and Eng. Aspects*, 80 (1993) 63.
13. E. Egorova, A. *Revina, Colloids and Surfaces A: Physicochem. and Eng. Aspects*, 168 (2000) 87.
14. R. Zhou, X. Wu, X. Hao, F. Zhou, H. Li, W. Rao, *Nuclear Instruments and Methods in Physics Research Section B: Beam Interactions with Materials and Atoms*, 266 (2008) 599.
15. J.N. Solanki, R. Sengupta, Z. Murthy, *Solid State Sciences*, 12 (2010) 1560.
16. P. Dash, *Research J. of Nanoscience and Nanotech.*, 1 (2010) 25.
17. K. Tian, C. Liu, H. Yang, X. Ren, *Colloids and Surfaces A: Physicochem. and Eng. Aspects*, 397 (2012) 12.
18. C. Rao, G. Kulkarni, V.V. Agrawal, U.K. Gautam, M. Ghosh, U. Tumkurkar, *J. of colloid and interface science*, 289 (2005) 305.
19. V. Pol, A. Gedanken, J. Calderon-Moreno, *Chem. of materials*, 15 (2003) 1111.
20. M. Möller, J.P. Spatz, A. Roescher, *Advanced Materials*, 8 (1996) 337.
21. M. Singh, I. Sinha, M. Premkumar, A. Singh, R. Mandal, *Colloids and Surfaces A: Physicochem. and Eng. Aspects*, 359 (2010) 88.
22. S. Joshi, S. Patil, V. Iyer, S. Mahumuni, *Nanostructured materials*, 10 (1998) 1135.
23. J. Hu, T.W. Odom, C.M. Lieber, *Accounts of chemical research*, 32 (1999) 435.
24. S. Goel, F. Chen, W. Cai, *Small*, 10 (2014) 631.
25. S. Mandal, S. De, *Colloids and Surfaces A: Physicochem. and Eng. Aspects*, 467 (2015) 233.
26. E.C. Hurdis, H. Romeyn, *Anal.Chem.*, 26 (1954) 320.
27. K. Sunil, B. Narayana, *Bulletin of environmental contamination and toxicology*, 81 (2008) 422.
28. Y.-z. Li, A. Townshend, *Analytica chimica acta*, 359 (1998) 149.
29. S. Xu, B. Peng, X. Han, *Biosensors and Bioelectronics*, 22 (2007) 1807.
30. B. X. Li, Z. J. Zhang and Y. Jin, *Sensor. Actuat. B: Chem.*, 72 **(**2001) 115.
31. A.A. Ensafi, M.M. Abarghoui, B. Rezaei, *Sensors and Actuat. B: Chem.*, 196 (2014) 398.
32. Y. Zhong, Y. Li, S. Li, S. Feng, Y. Zhang, *RSC Advances*, 4 (2014) 40638.
33. H. Lee, G. Lee, N. Jang, J. Yun, J. Song, B. Kim, *Nanotechnology*, 1 (2011) 371.
34. D. Majumder, *Inter. J. of Eng. Science and Technology*, 4 (2012) 4380.
35. A.A. Athawale, P.P. Katre, M. Kumar, M.B. Majumdar, *Materials chem. and physics*, 91 (2005) 507.
36. W. Li, M. Zhang, J. Zhang, Y. Han, *Frontiers of Chem. in China*, 1 (2006) 438.
37. S. De, S. Mandal, *Colloids and Surfaces A: Physicochem. and Eng. Aspects*, 421 (2013) 72.
38. S. Yokoyama, H. Takahashi, T. Itoh, K. Motomiya, K. Tohji, *Advanced Powder Technology*, 25 (2014) 999.

39. P. Kanhed, S. Birla, S. Gaikwad, A. Gade, A.B. Seabra, O. Rubilar, N. Duran, M. Rai, *Materials Letters*, 115 (2014) 13.
40. S.-Y. Deng, G.-Y. Zhang, D. Shan, Y.-H. Liu, K. Wang, X.-J. Zhang, *Electrochimica Acta*, 155 (2015) 78.
41. M. Amin, F. Anwar, M.R.S.A. Janjua, M.A. Iqbal, U. Rashid, *Inter. J. of molecular sciences*, 13 (2012) 9923.
42. J.P. Ruparelia, A.K. Chatterjee, S.P. Duttagupta, S. Mukherji, *Acta Biomaterialia*, 4 (2008) 707.
43. G. Applerot, A. Lipovsky, R. Dror, N. Perkas, Y. Nitzan, R. Lubart, A. Gedanken, *Advanced Functional Materials*, 19 (2009) 842.
44. R. Memming, *J.of The Electrochemical Society*, 116 (1969) 785.
45. P. Wu, P. Du, H. Zhang, C. Cai, *Physical Chemistry Chemical Physics*, 15 (2013) 6920.